

Magnetic and Dielectric studies of Ni-Co-Zn Ferrites synthesized by Non-conventional combustion method

Kavitha.N^{1*}, Manohar.P¹

¹Department of Ceramic Technology, A.C. Tech campus, Anna University, Chennai-600025, India

Abstract: Ni-Co-Zn Ferrites with the composition $\text{Ni}_{0.80-x}\text{Co}_x\text{Zn}_{0.20}\text{Fe}_2\text{O}_4$ ($x = 0.10, 0.20, 0.30, 0.40$) were synthesized by flash combustion method followed by calcinations at 900°C . Prepared samples were subjected to various characterization techniques such as X-ray diffraction (XRD), Fourier Transform Infrared Spectroscopy (FTIR), Vibrating Sample Magnetometer (VSM), and dielectric studies. XRD pattern shows that the prepared samples possess single phase spinel cubic structure and the particle sizes were calculated using Debye-Scherrer formula and the estimated particle size ranges 60–80 nm. FTIR studies also confirm the formation of spinel structure by having tetrahedral and octahedral modes of vibration bands between 400 and 600 cm^{-1} . Room temperature VSM studies shows the saturation magnetization values of prepared samples ranges between 55 and 68 emu/g. The increase in coercivity is observed due to the increase in anisotropy with the cobalt ion addition. The impedance measurements were carried out in the frequency range from 1 kHz to 5 MHz at room temperature. The Cole-Cole plot reveals the high resistive nature of the material and helps in analyzing the inherent phenomenon causes the conduction mechanism. The electrical and magnetic properties of Ni-Co-Zn ferrites were studied with respect to composition.

Key Words: Ni-Co-Zn Ferrites, combustion method, Magnetic properties.

Introduction

Ferrites are magnetic ceramic materials which are used in many applications such as core of transformer, recording heads, antenna rods, high quality filters, microwave devices, computer memory, logic devices, and many biomedical applications [1–4]. Ferrites are generally crystallized into spinel, garnet, magnetoplumbite, and orthoferrites. Each ferrite material is having unique properties which are required for a specific application. On the basis of magnetization, ferrites can further be classified in to soft and hard ferrites.

Among the soft ferrites, Ni-Zn ferrites are most versatile, technologically important materials which are used in high-frequency applications because of their high resistivity and low eddy current losses [5, 6]. Ni-Zn ferrites possess spinel cubic structure where they crystallize into four interpenetrating face-centered cubic closed packed structure of oxygen ions. In this structure, cations occupy two interstitial positions called as tetrahedral (A) and octahedral (B) sites. The properties of Ni-Zn Ferrites mainly depend on its distribution of cations in the A and B sites of spinel crystal structure, Synthesis methods, doped cations and its microstructure, etc., [7,8]. Among these factors, chemical composition plays important role in deciding its magnetic and electric properties and incorporation of new elements results in multi-component system which enhances their properties [9].

Ni-Zn ferrites can be synthesized by many methods such as solid state reaction [10], sol-gel [11], co-precipitation [12], reverse micelle technique [13], hydrothermal [14], and combustion method [15]. The selection of proper method for the synthesis depends on the desired properties and applications. Combustion method is chosen for the synthesis of Ni-Zn ferrites due to much simple processing steps, fast and inexpensive process, which results in nano-sized homogeneous pure ferrite powder [16]. By incorporating new elements in the place of nickel ion, the properties of Ni-Zn ferrite can be tailored and studied.

In this paper, a work is done on the synthesis and characterization of Co^{2+} ions substituted Ni-Zn ferrites and the effect of cobalt substitution on magnetic and dielectric properties were also studied.

Experimental method

Ni-Co-Zn ferrites with the composition of $\text{Ni}_{0.8-x}\text{Co}_x\text{Zn}_{0.2}\text{Fe}_2\text{O}_4$ ($x = 0.1, 0.2, 0.3, 0.4$) were synthesized using nickel nitrate, cobalt nitrate, Zinc nitrate, iron nitrate, and citric acid (fuel) as precursors. Stoichiometric amount of nitrates and citric acid were dissolved in the de-ionized water. Nitrates to citric acid ratio were maintained at 1 to obtain complete combustion. Citric acid-nitrate solution was kept in the stirrer which was at 80°C and stirred until it is transformed into a gel. The gel was transferred to the crucible and kept in the preheated furnace at 500°C . The combustion takes place within 5 minutes with large amount of fumes and results in burnt ash. Further the resultant ash was ground using mortar and pestle. The resultant fine powder was calcined at 900°C for 2 hours.

The calcined powder was subjected to various characterizations such as XRD, FTIR, and VSM. The pellets with the dimension of 12 mm diameter and 3 mm thickness were formed using 10 ton uniaxial press and were sintered at 1000°C for 2 hours. The sintered pellets were characterized to study the dielectric properties using LCR meter.

Results and discussion

XRD analysis:

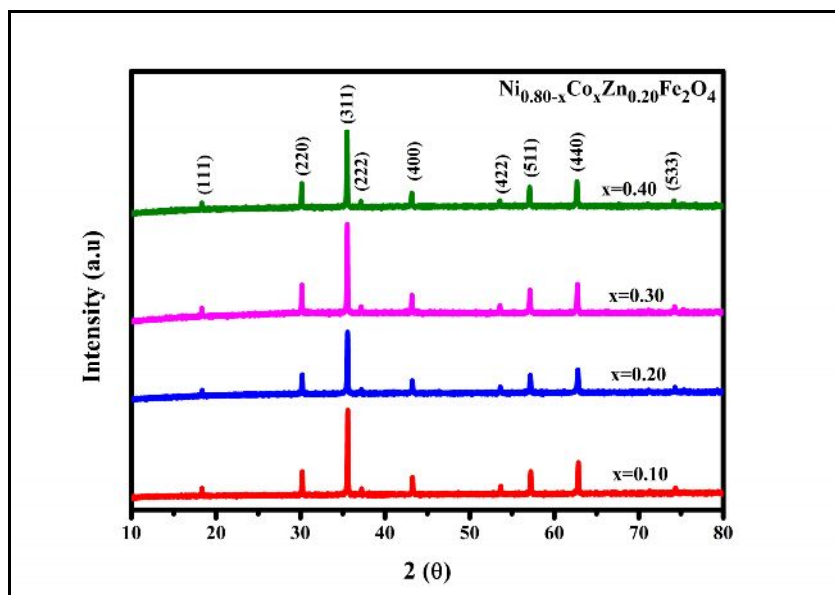


Figure (1) XRD pattern of $\text{Ni}_{0.80-x}\text{Co}_x\text{Zn}_{0.20}\text{Fe}_2\text{O}_4$ calcined at 900°C

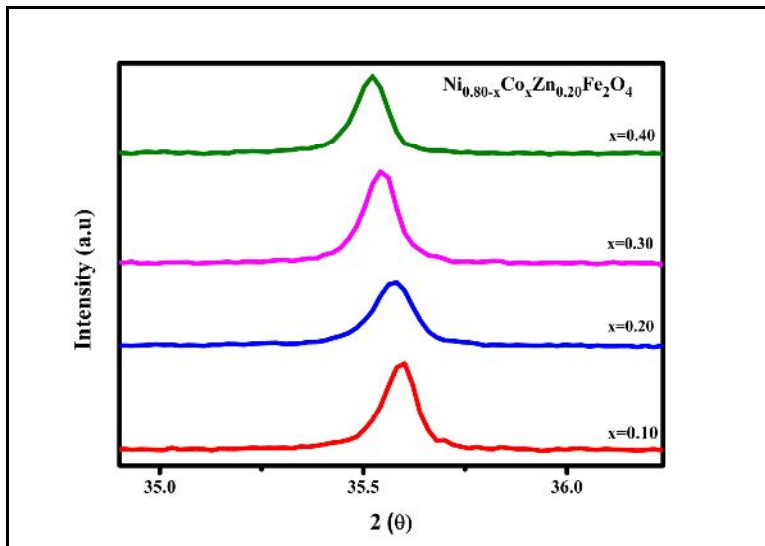


Figure 2 Shift of 2θ values with variation in cobalt concentration

Fig (1) shows the XRD pattern of prepared Ni-Co-Zn ferrites with different composition. All the samples show single phase highly crystalline spinel cubic structure. The XRD pattern can be well indexed with peaks corresponding to cubic spinel structure such as (111), (2 2 0), (3 1 1), (2 2 2), (4 0 0), (5 1 1), (4 4 0), and (5 3 3). This shows that the prepared sample has single phase spinel cubic structure. No other peaks corresponding to impurities or secondary phases were observed. The average crystallite size was calculated from the full width half maximum value of the reflection line (311) using Debye–scherrer formula,

$$D = 0.9\lambda / \beta \cos \theta$$

Where D is the average crystallite size, λ the wavelength of the X-ray, β the full width at half maximum of the reflection line, and θ the Bragg angle. The lattice constant (a) of all the samples were calculated using the relation,

$$a = d_{hkl} / (h^2 + k^2 + l^2)^{1/2}$$

where (hkl) are the miller indices and d_{hkl} is interplanar spacing. The X-ray density ($\rho_{X\text{-ray}}$) was calculated from the relation,

$$\rho_{X\text{-ray}} = 8M / Na^3$$

Where, M is the molecular weight, N the avogadro number and “a” is the lattice constant. The calculated values of crystallite size, lattice constant, d spacing, and X-ray densities are tabulated in Table (1). The calculated values are very well agreed with the results of different researchers.

Table (1) Variation of crystallite size, lattice constant, d-spacing, and X-ray density with cobalt ion concentration.

Co concentration	Crystallite size (nm)	Lattice constant (Å)	d spacing (Å)	X-ray density (g/cm ³)
x = 0.10	78.54	8.3577	2.5199	5.3579
x = 0.20	63.95	8.3613	2.5210	5.3502
x = 0.30	75.42	8.3684	2.5231	5.3372
x = 0.40	79.73	8.3736	2.5247	5.3278

As the cobalt concentration is increased there is an increase in lattice constant and d spacing which is because of the substitution of larger ionic radius Co^{2+} ions (0.72 Å) with Ni^{2+} ions (0.69 Å)[17,18]. X-ray density of the resultant powder decreases as the concentration of cobalt ion increases. From figure (2), we can

see that, incorporation of Co^{2+} ions in the place of Ni^{2+} ions shifts 2θ to lower angles, indicating corresponding increase in lattice parameter as the concentration is increased [9].

FTIR

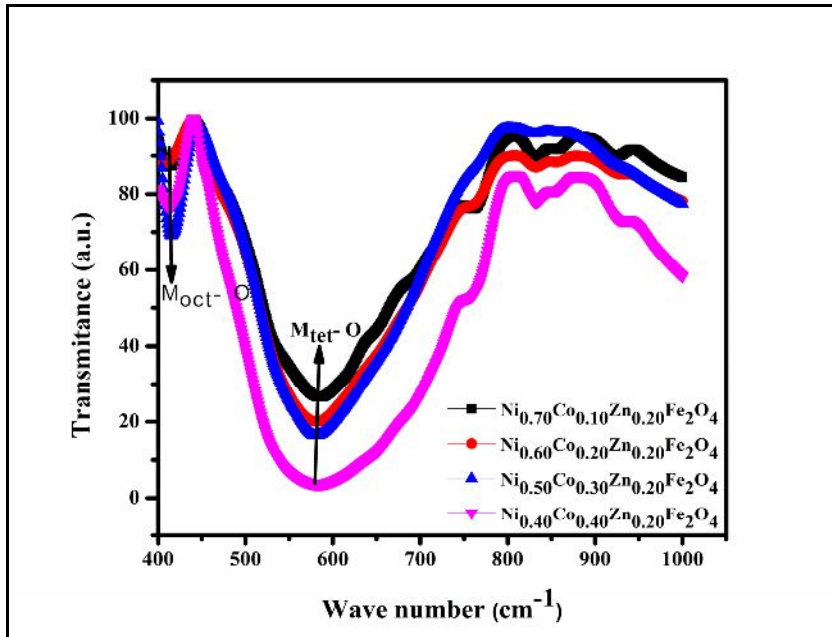


Figure (3) FTIR spectrum of $\text{Ni}_{0.80-x}\text{Co}_x\text{Zn}_{0.20}\text{Fe}_2\text{O}_4$

Figure (3) shows FTIR spectra recorded in the range of $400\text{--}1000\text{ cm}^{-1}$ for the samples with the composition of $\text{Ni}_{0.80-x}\text{Co}_x\text{Zn}_{0.20}\text{Fe}_2\text{O}_4$ (Where $x = 0.10, 0.20, 0.30, 0.40$). FTIR spectra show two important bands between 400 and 600 cm^{-1} which corresponds to the characteristic peaks of tetrahedral and octahedral mode of vibration of metal oxygen complexes in spinel ferrites [17]. The two different frequency bands arise because of the two different modes of vibration and its variation in bond lengths. The corresponding tetrahedral vibration frequency around $600(\nu_1)\text{ cm}^{-1}$ is due to the smaller bond length between metal–oxygen complexes. Similarly, the low frequency vibration at 400 cm^{-1} is due to the larger bond length between metal–oxygen complexes at octahedral position. The existence of two intrinsic peaks between 400 cm^{-1} and 600 cm^{-1} confirms the formation of the single phase spinel structure [19, 20].

VSM:

The room-temperature magnetic properties were studied from the VSM graph shown in the Figure (4). Room temperature values of saturation magnetization (M_s) and coercivity (H_c) are tabulated in the Table (2). All the samples show narrow hysteresis loop which indicates the soft ferrite nature. The resultant saturation magnetization values are decided by the distribution of cations in the tetrahedral (A) and octahedral (B) sites. The distribution of cations in the A and B sites are mainly decided by method of synthesis, sintering temperature, and type of cations, and so on. The super exchange interaction between A and B sites results in antiparallel spin alignment of cations. Hence, the resultant magnetization can be obtained from the difference between octahedral site magnetization (M_B) and tetrahedral site magnetization (M_A) [8]. The saturation magnetization (M_s) value increases as the concentration of cobalt ion increases except for the concentration $x = 0.30$.

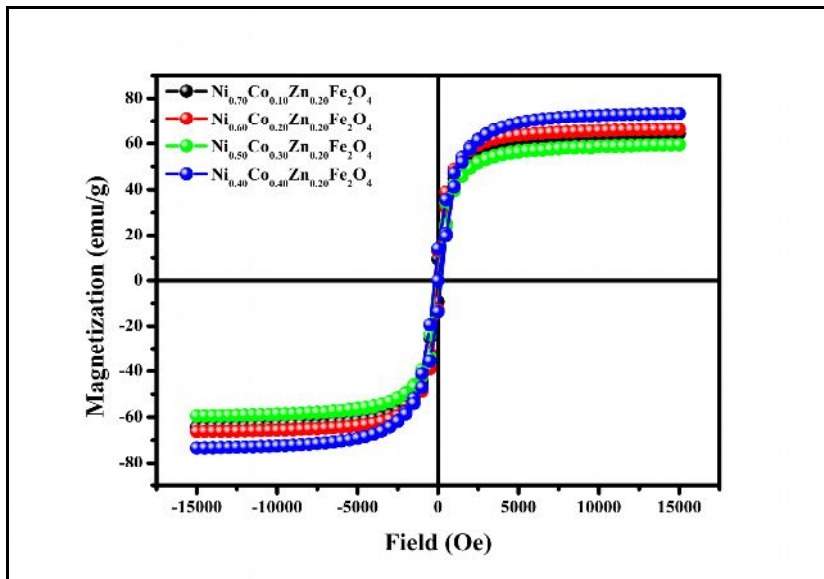


Figure (4) Room temperature hysteresis loop of calcined samples with varying cobalt content.

Co concentration	M_s (emu/g)	H_c (Oe)
x = 0.10	60.11	132.97
x = 0.20	62.74	145.60
x = 0.30	55.71	183.49
x = 0.40	67.60	208.75

The variation in saturation magnetization can be explained using Neel's two sub-lattice model. Cobalt ions with magnetic moment $3\mu_B$ have a preference to occupy octahedral (B) sites hence replaces nickel ions with magnetic moment $2\mu_B$ in B site, increases the net magnetic moment of B sites. The strong exchange interaction between A and B sites results in net increase in the saturation magnetization value with the increase in cobalt content except for $x = 0.30$. The decrease in the saturation magnetization for the concentration $x = 0.30$ may be due to the redistribution of cations among the available A and B sites which reduces A–B interaction [8,17]. It is observed that coercivity value increased from 132 to 208 Oe with the increase in cobalt content. This can be attributed to the enhancement of magnetocrystalline anisotropy with the introduction of more amounts of Cobalt ions [21].

Dielectric study

Impedance spectroscopy is used to study the dielectric properties of ferrites which give the details about the contribution of grain, grain boundary, and interface effect on its electrical properties over wide range of frequencies [22]. The graph plotted between real and imaginary part of impedance (cole-cole plot or Nyquist plot) gives the details about experimental data for the dielectric constant of many materials as a function of frequency [23].

Figure (5) shows the complex impedance spectra of Ni-Co-Zn ferrite samples prepared with different composition. For all the samples single incomplete semicircle was obtained due to the presence of multiple electrical responses [24]. This suggests that the grain interior contribution is not resolved for these samples and the prominent contribution is from grain boundary. It can be said in another way that the interior grain and grain-boundary contribution cannot be separated due to the presence of some additional time constants which occur outside the measured frequency range. The change in size of the semicircles can also be related to variation in grain size [25, 27].

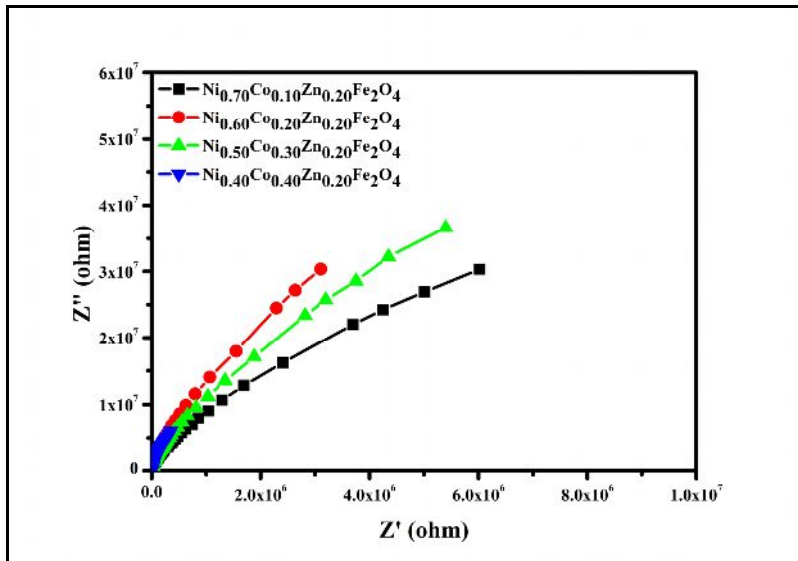


Figure (5) Cole-Cole plot of $\text{Ni}_{0.80-x}\text{Co}_x\text{Zn}_{0.20}\text{Fe}_2\text{O}_4$

The dielectric constant is calculated using the relation,

$$\varepsilon' = Ct/\varepsilon_0 A$$

Where, C is the capacitance, t the thickness of the pellet, A the area of cross section, ε_0 the permittivity of free space (8.85×10^{-14} (F/cm)).

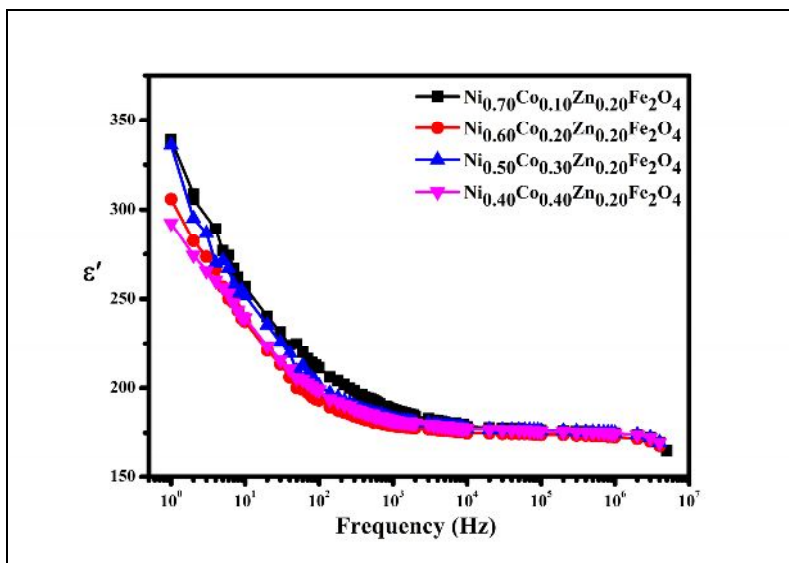


Figure (6) Variation of dielectric constant with frequency for $\text{Ni}_{0.80-x}\text{Co}_x\text{Zn}_{0.20}\text{Fe}_2\text{O}_4$.

Figure (6) shows graph between dielectric constant and frequency. Dielectric constant shows the usual dispersion behavior in low-frequency region and becomes constant at high-frequency region which attributes to the Maxwell–Wagner type interfacial polarization along with Koop's phenomenological theory. According to this theory, prepared samples can be assumed to possess a two-layer model. The first layer comprising of conducting grains and the layer which separates the grains are considered as a second layer being the highly resistive grain boundaries. This model results in accumulation of charge carriers near the resistive grain boundaries which leads to space charge polarization at lower frequencies. At higher frequencies, polarization cannot follow the applied alternating field as a result dielectric constant becomes constant at higher frequencies [26, 27].

The variation of dielectric constant with cobalt-ion concentration is also represented in the Figure (6). In general, the dielectric constant value is high for the material where the polarization is high. The dielectric constant strongly depends upon porosity, nature of crystallinity, pore-size distribution within the microstructure, and presence of same element with different valance states [28]. As the cobalt-ion concentration increases, at low frequencies dielectric constant value follows decreasing trend except for the concentration $x = 0.30$. This decrease can be attributed to the reduction in the species contributing for polarization decreases as the cobalt concentration increases. For $x = 0.30$ concentration of cobalt ion, there may be formation of more number of Fe^{2+} ions during sintering which results in excess Fe^{2+} and Fe^{3+} ion pairs where the hopping of electrons between these ions leads to high dielectric constant value[26,29].

Conclusions

Ni-Co-Zn ferrites with different concentrations of cobalt ions were synthesized using combustion method with subsequent calcinations at $900^{\circ}C$. The incorporation of cobalt ions in the spinel lattice and the formation of single phase were confirmed using XRD and FTIR studies. From VSM studies, the effect of cobalt substitution on saturation magnetization and coercivity was analyzed. It showed that there is an increase in saturation magnetization for all the concentration of cobalt ions except for $x = 0.30$ concentration and were explained using Neel's two sublattice model. The variation at $x = 0.30$ corresponds to the site preference of available cations which results in reduction of saturation magnetization value. The increase in coercivity with cobalt ion content can be related to the increased anisotropic nature of introduced cobalt ions. Cole-Cole plot suggests the high resistivity of the prepared samples by having single incomplete semicircle. The high dielectric constant value and its variation with frequency can be explained using the concept that all the samples possess two layers called conductive grain and high-resistive grain boundaries. Dielectric constant decreases as the cobalt concentration is increased except for $x = 0.30$. The rise in dielectric constant for the case of $x = 0.30$ concentration can be attributed to the formation of excess number of Fe^{2+} ions during sintering. This results in excess number of Fe^{3+} and Fe^{2+} ion pairs making the material more polarizable; hence, net increase in dielectric constant. Prepared materials' high magnetization, low coercivity, and high resistivity suggest that all the prepared materials can be used in high-frequency applications and high-density data storage devices.

References

1. Ch. Sujatha,n, K. Venugopal Reddy, K. Sowri Babu, A. Rama Chandra Reddy,M. Buchi Suresh, K.H. Rao. Effect of co substitution of Mg and Zn on electromagnetic properties of NiCuZn ferrites. *Journal of Physics and Chemistry of Solids*. 2013, 74; 917–923.
2. Amna Hassan, Muhammad Azhar Khan, Muhammad Shahid, M.Asghar, Imran Shakir, Shahzad Naseem, saira Riaz, Muhammad Farooq Warsi. Nanocrystalline $Zn_{1-x}Co_{0.5x}Ni_{0.5x}Fe_2O_4$ ferrites: Fabrication via coprecipitation route with enhanced magnetic and electrical properties. *J. magnetism and magnetic materials*,. 2015, 393; 56-61.
3. M.A.Gabal, W.A.Bayoumy, A.Saeed, Y.M.Al Angari. Structural and electromagnetic characterization of Cr- substituted Ni-Zn ferrites synthesized via egg white route.*J.Molecular structure*,. 2015, 1097; 45-51.
4. Lavanya Khanna, N.K.Verma. Synthesis, characterization and in vitro cytotoxicity study of calcium ferrite nanoparticles. *Materials science in semiconductor processing*,. 2013, 16; 1842-1848.
5. R.V.Mangalaraja, S.Ananthakumar, Manohar.P, F.D.Gnanam. Direct current resistivity studies of $Ni_{1-x}Zn_xFe_2O_4$ prepared through flash combustion and citrate gel decomposition techniques. *Materials Letters*,. 2003, 57; 2662-2665.
6. R.V.Mangalaraja, S.Ananthakumar, Manohar.P, F.D.Gnanam. Magnetic, electrical and dielectric behaviour of $Ni_{0.80}Zn_{0.20}Fe_2O_4$ prepared through flash combustion technique. *J.Magnetism and magnetic materials*,. 2002, 253; 56-64.
7. Lezhong Li, Rui Wang, Xiaoqiang Tu, Long Peng. Structure and static magnetic properties of Ti-substituted NiZnCo ferrite thinfilms synthesized by the sol-gel process. *J.Magnetism and magnetic materials*,. 2014, 355; 306-308.
8. K.Raju, G.Venkataiah, D.H.Yoon. Effect of Zn substitution on the structural and magnetic properties of Ni-Co ferrites. *Ceramics International*,. 2014, 40; 9337-9344.
9. Jian-ming Gao, Zhi-kai Yan, Jing Liu, Mei zhang, Min Guo. Synthesis, structure and magnetic properties of Zn substituted Ni-Co-Mn-Mg ferrites. *Materials Letters*,. 2015, 141; 122-124.

10. Muhammad Ajmal, Asghari Maqsood. AC conductivity, density related and magnetic properties of $Ni_{1-x}Zn_xFe_2O_4$ ferrites with the variation of Zinc concentration. *Materials Letters*,. 2008, 62; 2077-2080.
11. Khalid Mujasam Bato, M.S. Abd El-Sadek. Electrical and magnetic transport properties of Ni-Cu-Mg ferrite nanoparticles prepared by sol-gel method. *Journal of alloys and compounds*,. 2013, 566; 112-119.
12. S.Modak, M.Ammar, F.Mazaleyret, S.Das, P.K.Chakrabarti. XRD, HRTEM and magnetic properties of mixed spinel nanocrystalline Ni-Zn-Cu-ferrite. *Journal of alloys and compounds*. 2009, 473; 15-19.
13. Sangeetha Thakur, S.C.Katyayal, M.Singh. Structural and magnetic properties of nano nickel-zinc ferrite synthesized by reverse micelle technique. *Journal of magnetism and magnetic materials*. 2009, 321; 1-7.
14. K.Sadhana,K.Praveena, S.Bharadwaj, S.R.Murthy. Microwave –Hydrothermal synthesis of $BaTiO_3+NiCuZnFe_2O_4$ nanocomposites. *Journal of alloys and compounds*. 2009, 472; 484-488.
15. P.Priyadharshini, A.Pradeep, G.Chandrasekaran. Novel combustion route of synthesis and characterization of nanocrystalline mixed ferrites of Ni-Zn. *Journal of Magnetism and magnetic materials*. 2009, 321; 1898-1903.
16. R.V.Mangalaraja, S.Ananthakumar, Manohar.P, F.D.Gnanam. Initial permeability studies of Ni-Zn ferrites prepared by flash combustion technique. *Materials science and engineering A*. 2003, 355; 320-324.
17. M.A. Amer , A.Tawfik , A.G.Mostafa , A.F.El-Shora , S.M.Zaki. Spectral studies of Co substituted Ni-Zn ferrites. *J. Magnetism and magnetic materials*. 2011, 323; 1445-1452.
18. J.S. Ghodake, R.C. Kambale, S.V. Salvi , S.R. Sawant, S.S. Suryavanshi. Electric properties of Co substituted Ni-Zn ferrites. *J.Alloys and compounds*. 2009, 486; 830-834.
19. M. Siva Ram Prasad, B.Rajesh Babu, K.V.Ramesh, K.Trinath. Structural and magnetic studies on Chromium substituted Ni-Zn nano ferrite synthesized by citrate gel auto combustion method. *J.Supercond Nov magn.*,. 2014, 27; 2735-2745.
20. Manoj M.Kothawale, R.B.Tangsali, G.K Naik, J.S.Budkuley. Characterization and magnetic properties of Nanoparticle $Ni_{1-x}Zn_xFe_2O_4$ Ferrites prepared using Microwave assisted Combustion method. *J.Supercond Nov magn.*,. 2012, 25; 1907-1911.
21. U.B.Shinde, Sagar E.Shirsath, S.M. Patange, S.P.Jadhav, K.M.Jadhav, V.L.Palani. Preparation and characterization of Co^{2+} substituted Li-Dy ferrite ceramics. *Ceramics International*.2013, 39; 5227-5234.
22. P.P. Hankare , R.P.Patil , U.B.Sankpal, K.M.Garadkar , R.Sasikala, A.K.Tripathi, I.S.Mulla. Magnetic, dielectric and complex impedance spectroscopic studies of nanocrystalline Cr substituted Li-ferrite. *Journal of Magnetism and Magnetic Materials*. 2010, 322; 2629–2633.
23. Samiha T. Bishay. Numerical Methods for the Calculation of the Cole-Cole Parameters. *Egypt. J. Sol.*,. 2000, 23; 179-188.
24. Ming-ru syue, Fu-jin Wei, Chan-shin Chou, Chao-ming Fu. Magnetic, dielectric, and complex impedance properties of nanocrystalline Mn-Zn ferrites prepared by novel combustion method. *Thin solid films*,. 2011, 519; 8303-8306.
25. A.C.Druc, A.I.Borhan, G.G.Nedelcu, L.Leonite, A.R.Iordan, M.N.Palamaru. Structure-dielectric properties relationships in copper-substituted magnesium ferrites. *Materials Research Bulletin*,. 2013, 48; 4627 -4654.
26. Ibertombi soibam, Sumitra phanjoubam, H.B. Sharma, H.N.K. Sarma, Radhapiyari Laishiram, Chandra praksh. Effects of Cobalt substitution on the dielectric properties of Li-Zn ferrites. *Solid state communications*,. 2008, 48; 399-402.
27. A.C.Druc, A.I.Borhan, A.Diaconu, A.R.Iordan, G.G. Nedelcu, L.Leontie, M.N.Palamaru. How cobalt ions substitution changes the structure and dielectric properties of magnesium ferrite. *Ceramics International*,.2014, 40; 13573-13578.
28. K.Sudalai Muthu, N.Lakshminarasimhan. Impedance spectroscopic studies on $NiFe_2O_4$ with different morphologies: Microstructure Vs. dielectric properties. *Ceramics International*. 2013, 39; 2309-2315.
29. Gangadharan Sathishkumar, Chidambaram Venkataraju, Kandasamy sivakumar. Synthesis, Structural and Dielectric studies of Nickel substituted Cobalt – Zinc Ferrite. *Materials Sciences and Applications*. 2010, 1; 19-24.
